ELSEVIER

Polymer 40 (1999) 407–417

polymer

Effect of counter ions in electrochemical polymerization media on the structure and responses of the product polyaniline films
III. Structure and properties of polyaniline films prepared via electrochemical polymerization

Hikaru Okamoto*, Tadao Kotaka

Graduate School of Engineering, Toyota Technological Institute, 2-12-1 Hisakata, Tempaku, Nagoya 468, Japan

Received 27 November 1997; revised 13 January 1998; accepted 18 March 1998

Abstract

Using polymerization solutions containing 0.1 M aniline and 1 M HCl or 1 M $HClO_4$, which happened to give the same pH (0.2), we investigated the effects of different counter-anions on the primary and higher order structures as well as on electrochemical responses of the obtained polyaniline (PAn) films. From time developments of polymerization current and u.v.–visible absorption spectra as well as the results of atomic force microscopic (AFM) observation, we found that in both media the higher order structure of the PAn films developed in almost the same manner from grainy to fibrillar texture and finally to bundles of the fibrils. The primary structures as judged from the spectra were not very different, but the structural size was somewhat larger for the films prepared in $HClO_4$ than the ones prepared in HCl. The apparent acid dissociation constants of the resulting PAn films were again not so different, reflecting little differences in their primary structures. However, the electrochemical responses of the former were much slower than those of the latter, especially when the transition from the oxidation to reduction form was compared, reflecting differences especially in the structural size and compactness of their higher order structures.

Keywords: Polyaniline; Doping anion; Slow relaxation

1. Introduction

The recent surge of active interest in conducting polymers such as polyaniline (PAn) has been directed to the development of electronic and electrochromic devices [1–4] by utilizing its features in reversible doping/dedoping reactions and the changes in conductivity and/or absorption spectra upon potential switching. To obtain a high performance PAn film, it is essential to fabricate the polymer into a thin film of well-defined structure, preferably with a large surface area, which makes its response faster and more effective. For the preparation of such a film, electrochemical polymerization is a standard procedure. In such studies, a number of researchers reported that PAn films polymerized under different conditions possessed not only different primary structure but also different gross morphology [5–9], which thus exhibited different properties and responses [10,11].

In the electrochemical polymerization of aniline [12,13], nucleation takes place on a fresh surface of the electrode and the deposited PAn chains play a role of a newly formed surface for the subsequent growth. Thus the characteristics of the deposited PAn film, e.g. acid dissociation constant (pK_a) and conductivity, dominate the subsequent polymerization. The situation is in a sense similar to the metal electroplating process [14]. However, in the case of electrochemical deposition of PAn chains the surface characteristics may change as the deposition proceeds, as opposed to metal electroplating process [14] in which a fresh metal surface of the same characteristics is always created. Thus for the understanding of the electrochemical polymerization process of aniline, it is indispensable to examine development of both structure and characteristics of the film throughout a whole course of the polymerization, which is the main objective of this series of studies [15–17].

In fact, in this series of studies, we devised several novel methods of in situ characterization of growing PAn chains and examined the whole course of the electrochemical polymerization. The methods devised were time-resolved u.v.–visible (u.v.–vis) absorption spectrometry

* Corresponding author.

0032-3861/98/$ - see front matter
PII: S0032-3861(98)00248-1

and chrono-amperometry/potentiometry (CA/CP) to monitor, in effect, the development of the primary structure [15]. In particular, to monitor the gross morphology development, we incorporated a time-resolved low-angle laser-light scattering (LLS) photometry into our electrolysis system [16]. The gross morphology observation in the real space was conducted also by in-situ and/or out-of-situ atomic force microscopy (AFM) [16].

In the preceding paper [16] of this series, we conducted observation of the structure development in the course of electrochemical polymerization of aniline in the mixture containing 0.1 M aniline in 1 M HCl solution of pH = 0.2 via a constant potential mode at 0.73–0.79 V and confirmed that the primary structure of the PAn chains, as revealed by u.v.–vis spectra and the apparent acid-dissociation constants $(pK_a)_{app}$, was essentially unchanged with time, but the gross morphology developed from grainy texture to fibrillar aggregates of the grains and finally into bundles of the fibrils. The changes in the gross morphology should certainly accompany some changes in their electrochemical responses.

A remaining issue is thus how the electrochemical properties of PAn films may develop during the course of the polymerization. Although the above observation was conducted on 0.1 M aniline in 1 M HCl acid, some other strong acids such as $HClO_4$ can also be used [5,6,9] as a supporting medium for the electrochemical polymerization of aniline. Then still another issue is how these different counter-anions may affect the structure and electrochemical responses of the resulting PAn films. In this paper, we describe our attempt at examining these problems. To avoid unknown factors which might affect the polymerization behaviour, we selected 1 M HCl or 1 M $HClO_4$ as the supporting acids. Fortunately, as we found that 1 M HCl and 1 M $HClO_4$ containing 0.1 M aniline gave the same acidity of pH $\approx$ 0.2, we expected that the effects of pH and the counter-anion concentration were negligible by using these acids. Below we will describe the results.

2. Experimental

2.1. Preparation and characterization of polyaniline films

Following the procedures mentioned in our previous papers [15,16], we prepared PAn films in an electrochemical u.v.–vis spectrometry (EC–u.v.) cell composed of an ITO glass working electrode (WE) and a Pt wire counter electrode (CE) via constant potential electrolysis mode at a potential between +0.73 and +0.79 V (vs Ag/Ag^+/saturated KCl reference electrode: RE). The recipe was 0.1 M aniline plus 1 M HCl or 1 M $HClO_4$, which gave the same pH $\approx$ 0.2. We monitored the amount of deposition by means of a u.v.–vis spectrophotometer (u.v.-160; Shimazu Seisakusho, Kyoto) or coulomb-meter (HF-201; Hokuto-Denko, Tokyo). Since it was difficult to measure the real film thickness deposited on WE in situ, we used absorption strength Abs_{obs} at 420 nm (which is said to correspond to the absorption due to polaron [18]) as an index of the deposition level.

In each run we conducted electrochemical polymerization by passing the current under a constant potential until the Abs_{obs} reaches a prescribed level of usually 0.6 (for the HCl system it took ~3000 s and for the $HClO_4$ system ~5500 s; cf. Fig. 2). Then we stopped the polymerization, took out the film on WE from the cell, rinsed it several times in pure water and subjected it to the subsequent tests. When the amount of deposition was too much, a part of or a whole deposited PAn film was peeled off from WE during this rinsing treatment. The peeled-off PAn fragments were scooped up onto a mica plate to observe its morphology via AFM. The characterization of deposited PAn films was carried out by employing chrono-amperometry/absorptiometry and out-of-situ AFM observation according to the procedures described in our previous papers [15,16].

2.2. Determination of apparent acid dissociation constant $(pK_a)_{app}$

The apparent acid dissociation constant $(pK_a)_{app}$ of PAn films was determined also by the method described in our previous paper [15]. In each case, a throughly rinsed PAn film on WE prepared either in 1 M HCl or 1 M $HClO_4$ was subjected to the test for determining $(pK_a)_{app}$ by observing absorbance Abs_{obs} at 600 nm, where the dynamic range was the widest, in a 0.1 M potassium phosphate buffer with HCl or KOH plus KCl to keep a constant chloride ion concentration to $[Cl^-]=1$ M. From the plot of $\log\{(Abs_{HA^+}-Abs_{obs})/(Abs_{obs}-Abs_A)\}$ vs pH with the absorbance Abs_{HA^+} and Abs_A of the fully protonated and deprotonated form at low and high pH, respectively, we estimated $(pK_a)_{app}$ as the pH where Abs_{obs} reaches a half of the total change or $(Abs_{HA^+}-Abs_{obs})/(Abs_{obs}-Abs_A)=1$. We also determined the slope (m) of the plot as a measure of the distribution of the backbone conjugation length. The details were described in our previous paper [15].

2.3. Evaluation of electrochemical responses

Electrochemical responses of the PAn films were compared by the two following methods. The one was a cyclic voltammetric–absorptiometric (CV–Abs) tests in which simultaneous measurements of current and absorption strength at 420 nm, Abs_{420nm}, were conducted upon potential sweep from − 0.2 V to + 0.8 V and back to − 0.2 V at a sweep rate of 10 mV/s. The potential sweep was repeated several times until a steady cyclic voltammogram (CV) and a cyclic absorption-strength (CA) profile were obtained (cf. Fig. 6). The other was chrono-absorptiometry or absorbance relaxation (AR) test, in which changes in the Abs_{420nm} were monitored at an interval of 0.1 s as a function of time after a potential jump between − 0.2 V and + 0.6 V

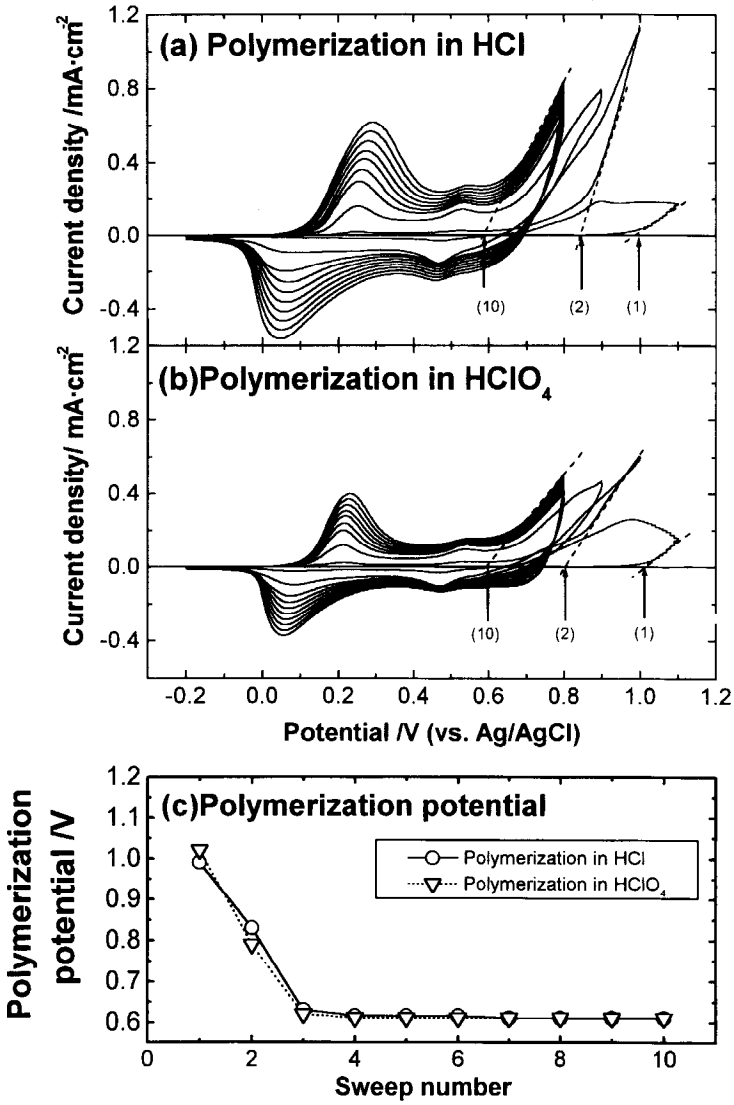

Fig. 1. First 10 scans of cyclic voltammograms (CV) of PAn films polymerized in (a) 1 M HCl and (b) 1 M $HClO_4$ in the early stages of polymerization, and (c) change of the polymerization potential with the sweep number. The CV scan was conducted by sweeping the potential at a rate of 20 mV/s for the first run from −0.2 to +1.1 V and back to −0.2 V, and for the second from −0.2 to +1.0 V and back, and afterwards between −0.2 and +0.8 V.

(cf. Fig. 7). In each run, first we kept a PAn film at − 0.2 V for about 5 min until the absorbance reached an apparent steady state, then switched to + 0.6 V and kept for another 30 s, and then stepped back to − 0.2 V, by observing the relaxation profile of the absorbance (cf. Fig. 7). The potential was controlled with a potentio/galvanostat with a function generator (HA-301/ HB-104; Hokuto-Denko, Tokyo) of which the response time was less than 15 μs.

We also conducted time-resolved double-step absorbance–relaxation (d-AR) tests on PAn films during the polymerization, in which we monitored changes in the absorbance at a two-step potential switching for the PAn film during the polymerization in the given medium. In this experiment, the potential was first kept at the polymerization potential of + 0.75 V for 120 s, switched down (the first step) to + 0.55 V and kept for 120 s where the polymerization was temporarily terminated but the PAn film was still in the oxidized coloured form, and then switched the potential down (the second step) to −0.2 V and kept for another 120 s to bring the film to the reduced colourless form, and then resumed again to +0.75 V to repeat the cycle. During these potential switching cycles changes in the absorbance at 420 nm was continuously monitored at an interval of 10 s (cf. Fig. 9). The cycle was repeated until the absorbance at +0.75 V ($Abs_{+0.75}$) finally reached to the saturation: $Abs_{+0.75} \approx 2$. The data were analysed by the method described later.

3. Results and discussion

3.1. Initiation of the electrochemical polymerization

First to compare the nucleation and polymerization

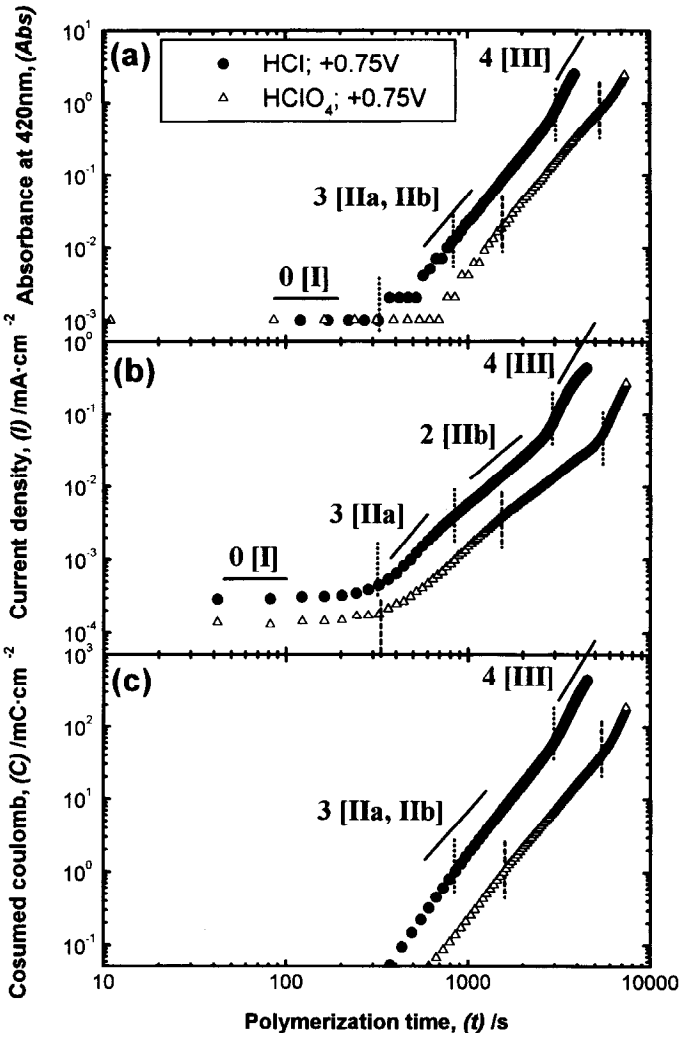

Fig. 2. Double logarithmic plots for developments of (a) absorbance at 420 nm (Abs_{420nm}); (b) electrolysis current (I) and (c) consumed coulombs (C) during the electrochemical polymerization at 0.75 V in 0.1 M aniline + 1 M HCl (solid circles) or 1 M $HClO_4$ (open triangles). Numerical symbols in the figures indicate values of n where *intensities* (Abs_{420nm}, I and C) $\propto t^n$.

potentials for the reaction mixtures of 0.1 M aniline in 1 M HCl and $HClO_4$, we conducted cyclic voltammetry or a potential sweep test in the very early stage of polymerization. Fig. 1 shows the first 10 cycles of voltammetric scan for (*a*) HCl and (*b*) $HClO_4$ systems. The scan was conducted in the potential range indicated in the caption with the scan rate of 20 mV/s. We see that in the first scan for the both systems the current began to flow indicating onset of the polymerization when the potential exceeded +1.0 V, obviously because the initiation or nucleation was driven by this over potential. As the scan was repeated, the potential at which the current began to increase, which we call the polymerization potential, shifts to the lower potential side. In Fig. 1(c) the polymerization potential is plotted against the scan number. We see that the potential rapidly decreases and levels out at + 0.6 V. Incidentally, we did not see any current increase if the potential was kept below + 0.6 V, which we thus called the polymerization threshold potential. Interestingly the plots are practically identical for both systems, implying that the difference in the counter-anion species does not affect the initiation and subsequent polymerization presumably until the electrode surface is covered with PAn chains. We thus selected a potential between +0.73 and 0.79 V for the subsequent experiments of the constant-potential mode polymerization.

3.2. Structure development during the polymerization

We prepared PAn films monitoring time-development of u.v.–vis spectra during the electrochemical polymerization at 25°C via a constant potential mode between + 0.73 and + 0.79 V for 0.1 M aniline in (a) 1.0 M HCl and (b) 1.0 M $HClO_4$ systems. For each of the systems, the spectral shape appeared not to change but the intensity constantly increases with the polymerization time.

Fig. 2 summarizes time-development of (*a*) the absorbance at 420 nm (*Abs*; proportional to the amount of PAn deposited), (*b*) the current density (I; proportional to the

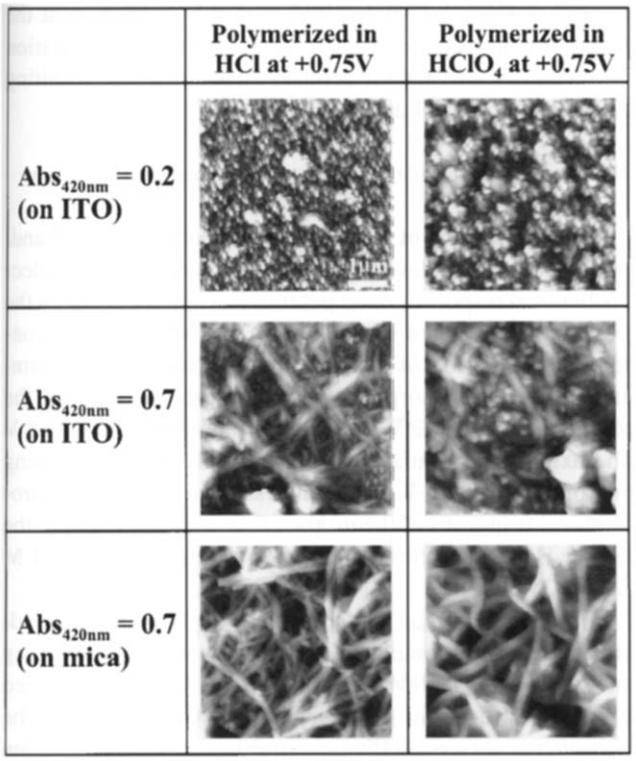

Fig. 3. Out-of-situ AFM images of PAn films polymerized in HCl (left column) and $HClO_4$ (right column), of which $Abs_{(420nm,\ +0.75)} = 0.2$ and 0.7.

polymerization rate) and (*c*) the consumed coulombs (*C*; again, proportional to the amount of PAn deposited) for the two systems polymerized at + 0.75 V. Time profiles of the curves are similar to each other, but the rates especially the nucleation rate is about twice faster in the HCl system than in the $HClO_4$ system, corresponding to the fact that the polymerization current in the initial CV scans develops much faster in the former than in the latter (cf. Fig. 1).

The similarity in the time development profiles of the absorbance (*Abs*) and current (*I*) leads us to speculate that structural developments and transitions in the two systems may also be the same: the initial region I (*Abs*, *I* and $C \propto t^0$) for the nucleation develops to the intermediate stages IIa and IIb ($I \propto t^3 \rightarrow t^2$, and *Abs* and $C \propto t^3$) for the grain- and fibril-formation and the final stage III (*Abs*, *I* and $C \propto t^4$) of the bundling of the fibrils, as discussed for the HCl system in a previous paper [16]. We thus characterized the morphology of the resulting PAn films via AFM. To do this, we stopped the polymerization at the different levels of $Abs_{420nm} \approx 0.2$ (the early stage of region IIb) and ≈ 0.7 (the late stage of region IIb), and subjected the films to the morphology observation via AFM. The results are shown in Fig. 3. At the level of $Abs_{420nm} \approx 0.2$, both films show a similar grainy texture of the size being smaller and of the appearance denser for the ones obtained from the HCl system than those from the $HClO_4$ system. On the other hand, the films at $Abs_{420nm} \approx 0.7$ level exhibit a grainy–fibrillar mixed texture of the size again smaller for the former than

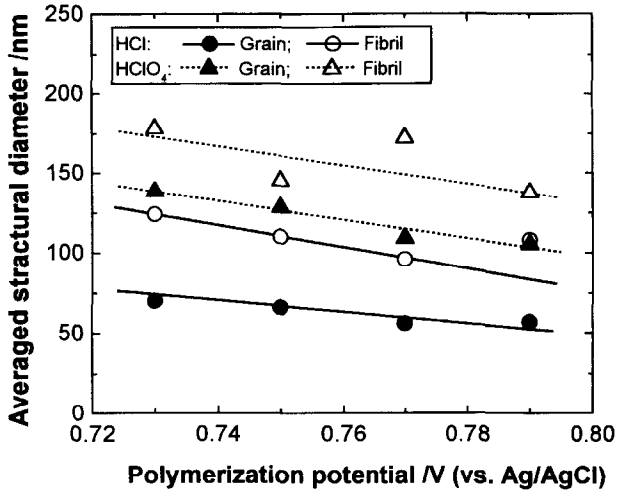

Fig. 4. Effects of acids (HCl or $HClO_4$) and applied potential on the structural size of the grains and fibrils of the resulted PAn chains via the constant potential mode polymerization.

that of the latter. From the PAn films at this $Abs_{420nm} \approx 0.7$ level, often fragments were peeled off from WE during the rinsing treatment. We scooped up the fragments onto a mica plate, and observed their morphology on AFM. Two pictures in the last row of Fig. 3 compare the AFM images, in which we see fibrillar textures.

For the PAn films polymerized at different potentials between +0.73 and 0.79 V, we confirmed that similar structural development and transition have taken place. However, the polymerization rate and the formed morphology were dependent on the applied potentials and the dopant anions. The polymerization in higher potentials and/or in HCl gave faster rates, and the structural size is smaller and the texture is more dense in the HCl system than those in the $HClO_4$ system. Fig. 4 summarizes the effect of the polymerization potential on the structural sizes of the grains and/or fibrils of the PAn films polymerized in the two systems. In each system, the higher polymerization potential leads to the films of a smaller size. The difference of the dopant anion on the structural size appears stronger than that of the applied potential. The structural sizes formed in $HClO_4$ at highest potential, +0.79 V, are still larger than those in HCl at lowest potential, +0.73 V.

The above observation of the structure developments as well as AFM observation of the PAn films polymerized in HCl and $HClO_4$ systems suggest that the structure develops in both systems more or less the similar manner starting from the initial nucleation stage I, the intermediate stages of grain (IIa) and fibril (IIb) formation and to the final stage of bundling of the fibrils. The rate of the structure development was by a factor of two to three slower in the $HClO_4$ system, but the resulted PAn films possessed somewhat larger structural size but with less compact aggregate structure, as compared with the ones obtained in the HCl system.

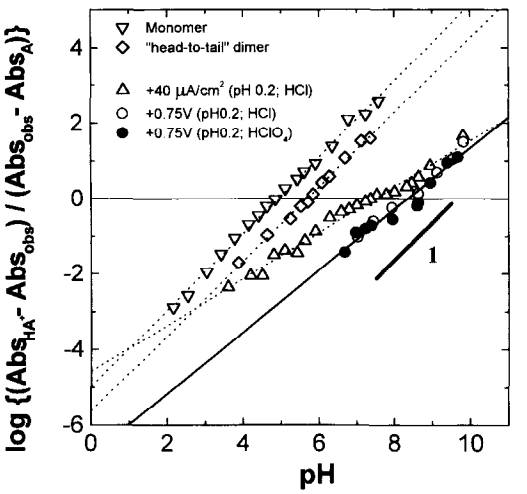

Fig. 5. Plots of $\log\{(Abs_{HA} - Abs_{obs})/(Abs_{obs} - Abs_{A})\}$ vs pH for aniline monomer, 'head-to-tail' dimer and PAn films polymerized under three different conditions as indicated.

3.3. Determination of apparent acid dissociation constants $(pK_a)_{app}$

To evaluate apparent acid dissociation constants, $(pK_a)_{app}$, which, we expected to provide a clue to understanding the difference, if exists, in the primary structure of the PAn chains in the films, we conducted pH titration experiments and analysed the u.v.–vis spectral data by the method proposed in our previous article [15]. From the changes of absorbance Abs_{obs} at an appropriate wavelength where the dynamic range of the absorbance was the widest, we constructed plots of $\log\{(Abs_{HA^+} - Abs_{obs})/(Abs_{obs} - Abs_{A})\}$ vs pH for the two PAn films, as shown in Fig. 5. For comparison, Fig. 5 also includes the same plots for aniline monomer and the 'head-to-tail' dimer, *N*-phenyl-*p*-phenylene-diamine (for pK_{a1} only), and also for a PAn film polymerized in 1 M HCl of pH = 0.2 under a constant current mode of 40 $\mu A/cm^2$.

From these plots shown in Fig. 5, we determined $(pK_a)_{app}$ and the slope m which is expected to reflect the distribution in the conjugation length of the PAn chains. Thus for a species having a single protonation/deprotonation site such as aniline the slope m should be close to 1. From these plots, we found that $(pK_a)_{app}$ and m were, respectively, 4.86 and 1.01 for aniline and 5.72 (for pK_{a1}) and 0.99 for the dimer, which are in good agreement with the literature values [19]. The determined $(pK_a)_{app}$ and m are, respectively, 8.32 and 0.85 for the PAn film polymerized in HCl, and 8.61 and 0.77 for the one in $HClO_4$. The differences in $(pK_a)_{app}$ and m between the two PAn films are trivial. Incidentally, the values determined for the film prepared via the constant current mode are $(pK_a)_{app} = 7.45$ and m as small as 0.47, reflecting the severe heterogeneity in the primary structure of their backbone conjugation.

In effect, we found virtually no difference in the u.v.–vis spectra, $(pK_a)_{app}$ and the slope m, which suggests that the different acids, HCl or $HClO_4$, used as the polymerization media hardly affected the primary structure of the resulting PAn films, if the pH are the same.

3.4. Electrochemical responses of the product PAn films

The performance of PAn films as an electrochemical and/or electrochromic device obviously depends on their electrochemical responses upon potential switching between the oxidized and reduced states. To see this behaviour we conducted observation of spectral change, and cyclic voltammetric (CV) and absorptiometric (CA) tests by sweeping the potential from − 0.2 V (the reduction potential) to + 0.8 V (the oxidation potential) and back usually with a sweeping rate of 10 mV/s to see difference/similarity in the electrochemical responses of the product PAn films prepared in the HCl or $HClO_4$ systems. These tests were conducted in 1 M HCl at 25°C.

Fig. 6 shows cyclic voltammetric (CV) and corresponding cyclic absorptiometric (CA) patterns with the sweeping rate of 10 mV/s in 1 M HCl for the PAn films polymerized at + 0.75 V from (*a*) the HCl and (*b*) $HClO_4$ systems. The CV patterns are essentially the same, but the CA patterns are significantly different for the two films especially in the amount of residual absorbance at the reduction potential of − 0.2 V, reflecting the difference in the spectra for the reduced films. This behaviour should reflect the differences of the two films in their response speeds or the rates of transition from the oxidized to the reduced state and vice versa.

To confirm the differences in their response speeds, we conducted chrono-absorptiometry on the PAn films recovered after the polymerization in HCl and $HClO_4$. In the CA-response test, we observed time profiles of the absorption strength at 420 nm, Abs_{420nm}, of the PAn films immersing them in 1 M HCl upon potential switching from − 0.2 to + 0.6 V for 30 s and then back again to − 0.2 V following the pattern illustrated in the top panel of Fig. 7. Fig. 7*a* shows the results on the films polymerized at four different potentials between +0.73 and +0.79 V in 1 M HCl, and Fig. 7*b*, those in $HClO_4$.

In Fig. 7 we notice that the absorbance always exhibits an overshoot upon potential switching up from −0.2 to +0.6 V or down from +0.6 to −0.2 V. A possible source of the overshoot is that, as seen in the CA diagrams shown in Fig. 6, the absorbance passes a peak at around ~0.4 V or at ~0.2 V when the potential is increased or decreased, respectively, from/to −0.2 V to/from +0.6 V, regardless of the scan speed. In other words, the potential switching is no other than a CA scan with an extremely rapid rate.

Another finding is the difference found in the absorbance decay rates between the oxidizing and reducing processes. The absorbance rapidly levels out to the steady state when the applied potential is switched up from the reduction to the oxidation state, but it does rather slowly when the potential

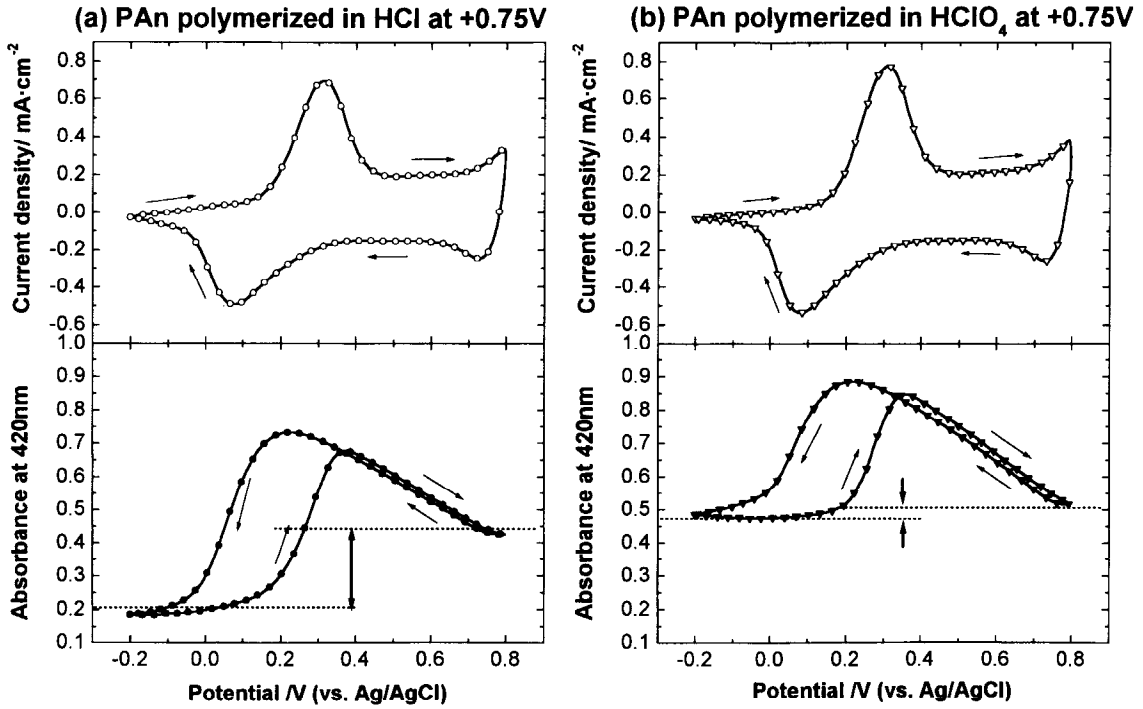

Fig. 6. Cyclic voltammograms (CV) and cyclic absorption strength (CA) profiles of PAn films subjected to 10 mV/s potential scanning in 1 M HCl. The PAn samples were prepared at + 0.75 V in 0.1 M aniline + 1 M (a) HCl or (b) $HClO_4$.

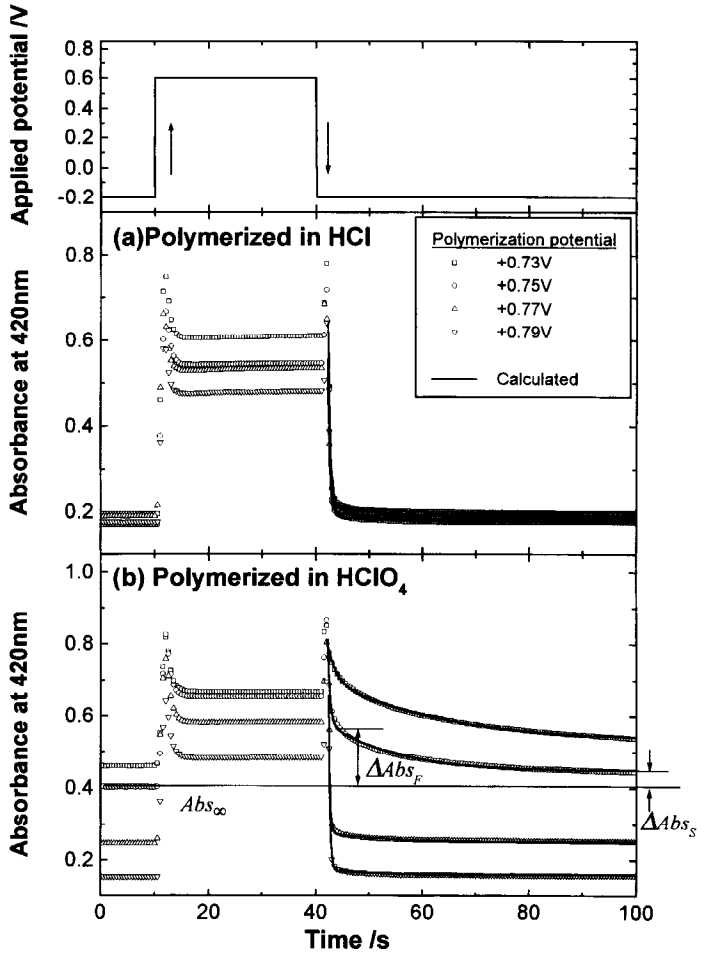

Fig. 7. Chronoabsorptiometry of PAn film polymerized in (a) HCl and (b) $HClO_4$ at + 0.73–0.79 V when the applied potential was switched from − 0.2 to +0.6 V and then to − 0.2 V again as depicted in the top panel. The solid lines show the results of nonlinear curve fitting with Eqs. (1) and (2).

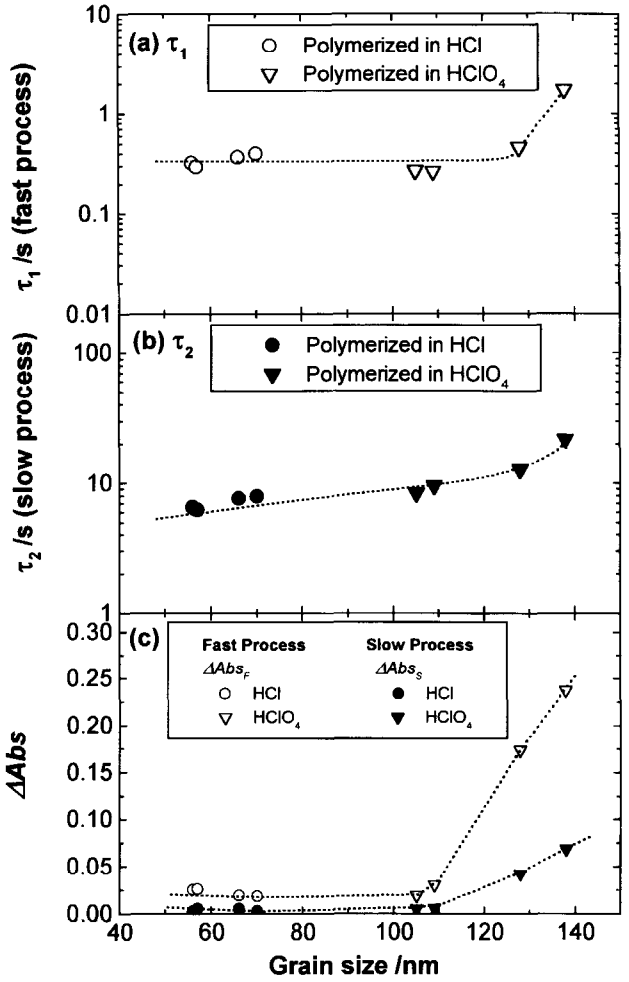

Fig. 8. Relationships between the grain size of PAn films prepared in each acid and (a) the relaxation time, τ_1, (b) τ_2 for the slow process, and (c) the corresponding residual absorbances, ΔAbs_F and ΔAbs_s.

is switched down to the opposite direction. This means that the latter is the rate determining process.

If the performance of the films prepared in HCl and $HClO_4$ systems are compared, we notice that $HClO_4$ films show poorer performance: the decay especially upon potential switching down is very slow for those prepared in $HClO_4$ as compared to those prepared in HCl, and the levels of initial absorbance, Abs_∞, and residual absorbance, ΔAbs_s (that should eventually vanish at $t \rightarrow \infty$), are considerably high as compared to those prepared in HCl.

We thus compared the absorbance decay behaviour of the PAn films especially in the potential switching-down process form + 0.6 V to − 0.2 V. In order to carry out a quantitative analysis, we introduce the following two- process model for the time profile of the absorbance upon potential switching:

$$Abs = Abs_0 + Abs_1[1 - \exp\{-(t - t_0)/\tau_1\}] + Abs_2[1 - \exp\{-(t - t_0)/\tau_2\}] \quad (1)$$

$$\Delta Abs_F = (Abs_0 + Abs_1) - Abs_\infty;$$

$$\Delta Abs_s = (Abs_0 + Abs_1 + Abs_2) - Abs_\infty \quad (2)$$

Here Abs_i and τ_i are the relaxation strength and time, respectively, for the fast ($i = 1$) and slow ($i = 2$) processes. The ΔAbs_F and ΔAbs_s are the residual absorbances after the fast and slow processes, respectively. Employing a software for nonlinear curve fitting and collecting data obtained ~0.90 s after the potential switching (to avoid complications due to the overshoot), we determined the values of these model parameters for all the absorbance decay curves. Fig. 8 summarizes the results as a function of the grain size (as estimated via AFM) for the relaxation times τ_1 and τ_2 and the residual absorbances ΔAbs_F and ΔAbs_s determined in 1 M HCl medium for the PAn films polymerized in the HCl (circles) and $HClO_4$ (triangles) systems.

Reflecting the differences in the grain size the data points for the former cover the smaller size and better performance range as compared to those of the latter belonging to the larger size and poor performance range. When the grain size exceeds ~100 nm level, the relaxation times become longer (or the response rates slower) and the amounts of dischargeable/rechargeable charges become smaller as judged from the levels of the residual absorbance become larger.

The same CA-response test was conducted on the two PAn films to compare their response by using 1 M $HClO_4$ as a test medium. Although we do not show the results here, the responses were slightly slower in $HClO_4$ than in HCl, but the effects of the grain size were essentially the same with those conducted in HCl. The results imply that the electrochemical responses are governed essentially by the acids used in the polymerization media (thus by the gross morphology of the films) but not much by those used in the CA-response test, if their primary structures are the same.

3.5. Changes in the performance of PAn films during electrochemical polymerization

The results in the preceding section clearly showed that the electrochemical responses of PAn films are dependent on the gross morphology especially on the grain size. We thus designed a time-resolved double-step absorbance–relaxation (d-AR) test or 'in-situ potential switching' test and attempted to follow the changes in the responses of PAn films with time in the polymerization media containing 0.1 M aniline in either 1 M HCl or 1 M $HClO_4$, both at pH ≈ 0.2, via a constant potential mode at +0.75 V. In this system, the polymerization proceeds at +0.75 V but below the critical or threshold polymerization potential of + 0.6 V, no polymerization takes place. Thus, in the d-AR test, we selected the potential switching pattern such as shown in Fig. 9*a*. In a typical cycle of this test, first the potential was kept at + 0.75 V for 2 min (the polymerization phase), then stepped down to + 0.55 V and kept for 2 more min (the stand-by phase) and then stepped down to −0.2 V and kept for another 2 min (the monitoring phase), and finally brought back to + 0.75 V to resume to the polymerization phase, through which changes in the absorbance at 420 nm were monitored at an appropriate interval.

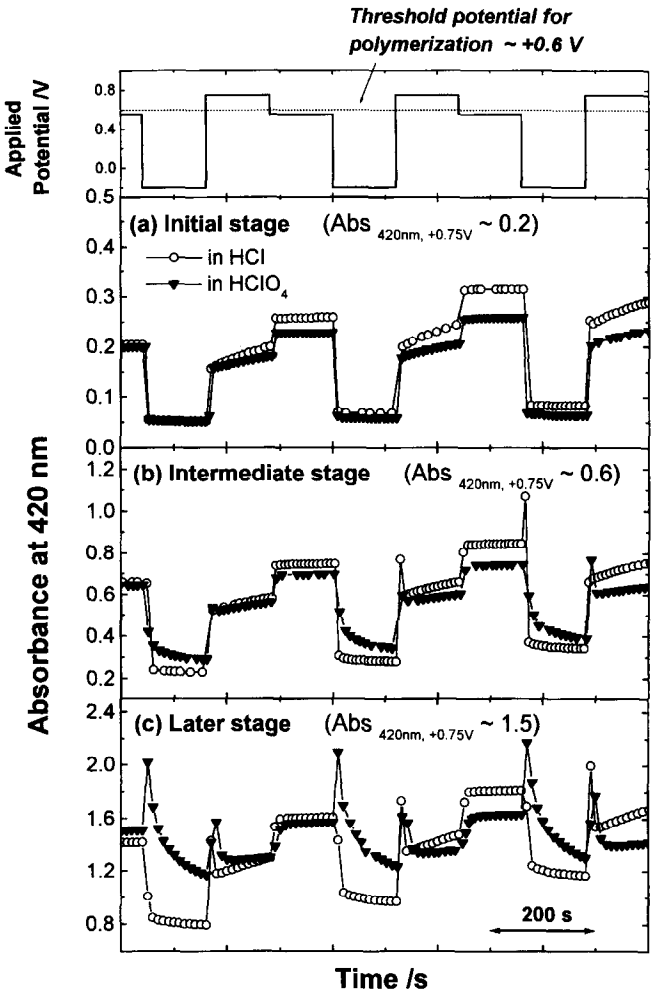

Fig. 9. Typical profiles of electrochemical responses upon potential switching (shown in the top panel; d-AR test) of PAn films in the polymerization media of HCl (open circles) or $HClO_4$ (closed triangles) in the different stages of polymerization. The real time spans were: (a) in the early stage, $t = 4300$–5300 s in HCl and 8260–9260 s in $HClO_4$; (b) in the intermediate stage, $t = 6820$–7820 s and 11 860–12 860 s; and (c) in the late stage, $t = 8980$–9980 s and 18 340–19340 s, respectively.

The potential switching pattern is illustrated in the top panel of Fig. 9, and in Fig. 9a–c typical absorbance–time profiles are compared for the PAn films during the polymerization in HCl (open circles) or in $HClO_4$ (closed triangles). Because the rates are different for the two systems, the profiles are compared at the similar levels of PAn deposition: in the early stage where the absorbance, $Abs_{420nm,+0.75V}$, is the order of ~0.2 OD unit, in the intermediate stage of *Abs* ~0.6 OD unit, and in the late stage of *Abs* ~1.5 OD unit, respectively. The amount of PAn deposition was evaluated as the absorbance at 420 nm, $Abs_{420nm,+0.75V}$, observed during the polymerization phase at + 0.75 V, and the d-AR profiles are compared at the same level of polymerization, as shown in Fig. 9. The absorbance profiles are obviously different for the two systems, and the difference increases with the amount of PAn deposition. The responses are apparently better for the HCl films with smaller grain size and more compact gross structure rather than for the $HClO_4$ films with larger grain size and less compact structure.

Whenever necessary, we stopped the polymerization by bringing the potential down to −0.2 V and subjected the growing PAn film to a test with a potential switching pattern similar to the AR test for the product PAn film (without aniline in the medium) except by keeping the high potential below +0.55 V (to avoid undesirable polymerization to take place), and the electrochemical responses were evaluated from the absorbance data obtained during the stand-by and monitoring phases at 0.1 s interval. The data were analysed with Eqs. (1) and (2) by the method described above to evaluate τ_1 and τ_2 and ΔAbs_F and ΔAbs_s for the transition from an oxidized state at +0.55 V to the reduced state at −0.2 V. Fig. 10 compares (*a*) τ_1 for the fast process, (*b*) τ_2 for the slow process, and (*c*) ΔAbs_F and ΔAbs_s for the HCl and $HClO_4$ systems. In Fig. 10 the abscissa is the absorbance, $Abs_{420nm,+0.75V}$, at 420 nm under +0.75 V that approximately reflects the amount of PAn deposited but not necessarily the true film thickness. We see in Fig. 10 that as long as τ_1 and ΔAbs_F are concerned, the performances of the either films do not change much during the intermediate stages IIa to IIb. The responses, however, become somewhat

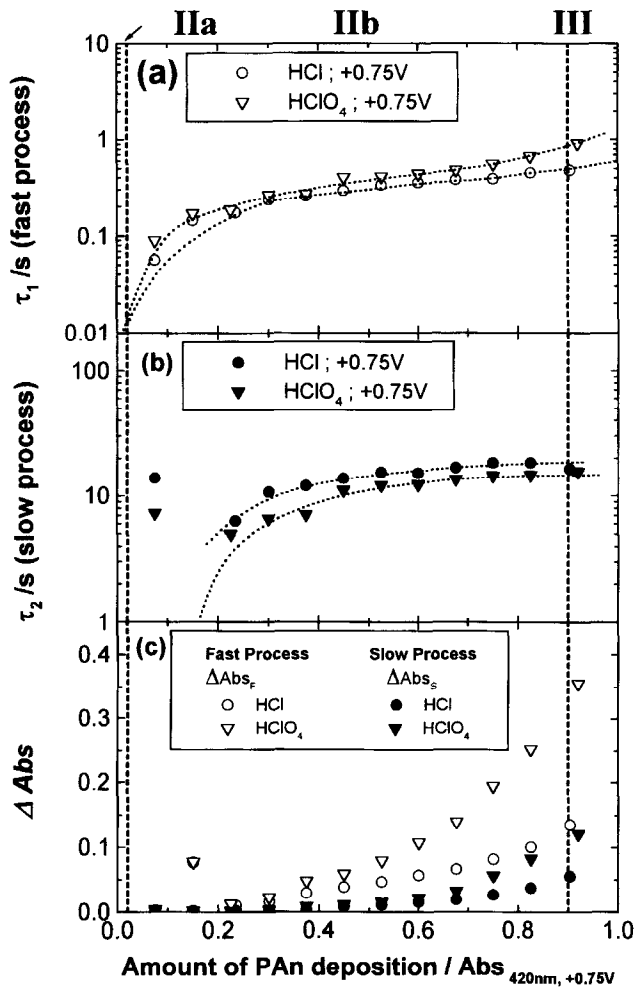

Fig. 10. Plots of (a) the relaxation time, τ_1, for the fast process, (b) τ_2 for the slow process, and (c) the residual absorbances, ΔAbs_F and ΔAbs_S against the amount of the growing PAn deposition evaluated as the absorbance $Abs_{420nm,+0.75V}$ under a constant potential mode polymerization at +0.75 V in HCl (circles) or $HClO_4$ (triangles).

slower and worse in the late stage III, especially for the $HClO_4$ system.

The results of u.v.–vis spectra and the apparent acid dissociation constant, $(pK_a)_{app}$, and the slope m, suggest that the primary structure is virtually the same in the two systems prepared in HCl and in $HClO_4$. Nevertheless, the electrochemical responses as judged from the absorbance–time profiles upon potential switching (cf. Figs 7, and 9) and the response rates and strengths (cf. Figs 8, and 10) are quite different. Thus the differences must reflect the differences in the higher order structure or the gross morphology of the PAn films prepared in the different acids.

First we notice that as judged from the transition rate from the oxidation-to-reduction state (a discharging process) are slower than the rate of the reverse process from the reduction-to-oxidation state (a charge-up process), the former is obviously the rate-determining process in their electrochemical responses. The similar behaviour was observed in many conducting polymers, and the phenomenon

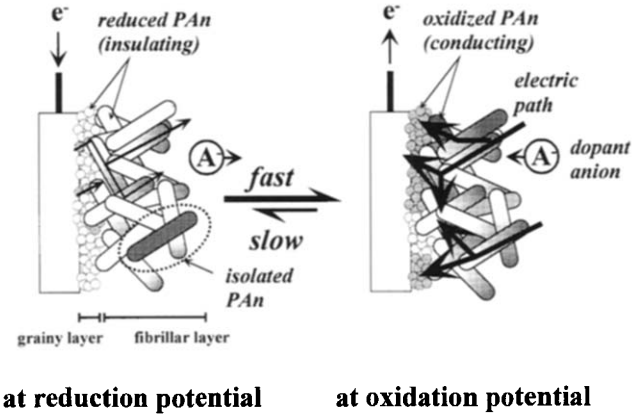

Fig. 11. A model depicting the gross morphology and slow electrochemical responses of PAn films.

was often called 'memory effect' or 'slow relaxation' and interpreted in several different ways [20–28] including a percolation model proposed by Aoki et al. [26–28].

If we introduce a structural model such as depicted in Fig. 11, which is quite likely in view of our structural analysis including AFM microscopy, the behaviour is quite understandable. When the potential is switched from the reduction to oxidation potential, the insulating-to-conducting transition of PAn develops from the proximity of the electrode surface toward the bulk phase, creating electric paths (percolation) to accelerate further transition. However, when the potential is switched down from the oxidation to reduction potential, the conducting-to-insulating transition occurs, reducing the electric paths to increase the impedance. As a result, this makes some charges trapped in isolated conducting domains of the grains and fibrils surrounded by those of the insulating phase through which trapped charges hardly diffuse away. This situation results in a u.v.–vis spectrum of mixed insulating and conducting phases even after a prolonged electrochemical reduction.

According to our previous paper [16], the IIb stage of the structure development corresponds to the growth process of fibrillar textures through aggregation of the grains produced in the IIa stage. In this stage IIb, bulk density becomes smaller with the growth of fibrillar textures as contrasted to the higher density of grainy textures appearing in the stage IIa. Under such a situation, an increased deposition of PAn chains into grains, fibrils and bundles of the fibrils with less compact structure, especially in those prepared in $HClO_4$ system, tends to increase the inter-chain, inter-grain, inter-fibrillar impedance of the PAn film, which tendency certainly should retard the relaxation or make the discharging slower and less complete.

Our model and the interpretation of the so-called 'memory effect' is compatible with the percolation model proposed by Aoki et al. [26–28] who interpreted this phenomenon as the slow relaxation being caused by competition between diffusional retrieval of electric paths from

the local conducting domains to the electrode and the electrochemical cutoff of the electric paths. In fact, our preliminary results on simultaneous measurement of CV and impedance at 10 kHz using an interdigitated array (IDA) electrode [17] showed that impedance of PAn films on IDA electrode was reduced by the electrochemical oxidation and between $\sim +0.2$ and $\sim +0.8$ V reached the lowest steady state value. In this potential range we found the cyclic absorptiometry (CA) diagram showed no hysteresis as seen in Fig. 6. Furthermore, the PAn films polymerized in $HClO_4$ gave faster impedance changes and larger values than those polymerized in HCl. These results reinforce our reasoning for the relaxation behaviour.

4. Conclusions

The PAn films polymerized in the media containing different counter anions, 1 M HCl or $HClO_4$ in this study, but with the same pH and concentrations possess almost the same primary structure and exhibit virtually the same development profiles of the higher order structure or gross morphology, although the rates of the development and the size and density of the structure of the obtained films are different. Presumably reflecting the differences in the higher order structure, they exhibited different electrochemical responses, especially when the applied potential was switched to induce transition from the oxidized, conducting phase to the reduced, insulating phase. This is due to the fact that this transition makes electric paths in PAn films decrease and then prevents further electrochemical reaction to take place. This tendency was particularly remarkable in the PAn films polymerized in $HClO_4$ under a low potential close to the polymerization threshold, which led to a PAn film of larger structural size but a less compact structure. The larger the structural size and the lesser the density of the grains and fibrils, the higher the impedance of their boundaries, which makes the trapped charges difficult to diffuse away.

References

[1] Osaka T, Ogano S, Naoi K, Oyama N. J Electrochem Soc 1989;136:306.
[2] Yonezawa S, Kanamura K, Takehara Z. J Electrochem Soc 1989;140:629.
[3] Kobayashi T, Yoneyama H, Tamura H. J Electroanal Chem 1984;161:419.
[4] Jelle BP, Hagen G. J Electrochem Soc 1993;140:3560.
[5] Huang Wu-Song, Humphrey BD, MacDiarmid AG. J Chem Soc Faraday Trans. I 1986;82:2385.
[6] Duić Lj, Mandić Z, Kovačiček F. J Polym Sci, Part A: Poly Chem 1994;32:105.
[7] Yan H, Toshima N. Hyomen 1995;33:295.
[8] Nunziante P, Pistoia G. Electrochim Acta 1989;34:223.
[9] Zotti G, Cattarin S, Comisso N. J Electroanal Chem 1988;239:387.
[10] Takei K, Ishihara K, Iwahori T, Tanaka T. Denki Kagaku (J Electrochem Soc Jpn) 1989;58:934.
[11] Osaka T, Ogano S, Naoi K, Oyama N. J Electrochem Soc 1989;136:306.
[12] Bade K, Tsakova V, Schultze JW. Electrochim Acta 1992;37: 2255.
[13] Córdova R, del Valle MA, Arratia A, Gómez H, Schrebler R. J Electroanal Chem 1990;377:75.
[14] Brett CMA, Brett AMO. Electrochemistry; principles, methods and applications. New York: Oxford University Press, 1994, p. 341.
[15] Okamoto H, Kotaka T. Polymer 1998;18:4349.
[16] Okamoto H, Okamoto M, Kotaka T. Polymer 1998;18:4359.
[17] Okamoto H, Ando Y, Kotaka T. Synthetic Metals 1998; in press.
[18] Stilwell DE, Park S-M. J Electrochem Soc 1989;136:427.
[19] Lide DR: ed. CRC handbook of chemistry and physics 1995–1996, 76th edn. Boca Raton, FL: CRC press, 1996: 8-43–8-55.
[20] Heinze J, Biler R, Meerholz K. Ber Bunsenges Phys Chem 1988;92:1266.
[21] Odin C, Nechtschein M. Phys Rev Lett 1991;67:1114.
[22] Odin C, Nechtschein M, Hapiot P. Synthetic Metals 1992;47:329.
[23] Kalaji M, Nyholm L, Peter LM. J Electroanal Chem 1992;325:269.
[24] Laridjani M, Pouget JP, Scherr EM, MacDiarmid AG, Jozefowicz ME, Epstein AJ. Macromolecules 1992;25:4106.
[25] Fraoua K, Delamar M, Andrieux CP. Synthetic Metals 1996;78:131.
[26] Aoki K. J Electroanal Chem 1994;373:67.
[27] Aoki K, Cao J, Hoshino Y. Electrochimica Acta 1994;39:2291.
[28] Aoki K, Kawase M. J Electroanal Chem 1994;377:125.